Atmos. Chem. Phys. Discuss., doi:10.5194/acp-2016-410, 2016
Manuscript under review for journal Atmos. Chem. Phys.
Published: 24 May 2016

Atmospheric Chemistry and Physics Discussions

Distribution and Sources of Air pollutants in the North China Plain Based on On-Road Mobile Measurements

Yi Zhu[1], Jiping Zhang[2], Junxia Wang[1], Wenyuan Chen[1], Yiqun Han[1], Chunxiang Ye[3], Yingruo Li[1], Jun Liu[1], Limin Zeng[1], Yusheng Wu[1], Xinfeng Wang[4], Wenxing Wang[4], Jianmin Chen[4], and Tong Zhu[1,5*]

[1]State Key Joint Laboratory of Environmental Simulation and Pollution Control, College of Environmental Sciences and Engineering, Peking University, Beijing 100871, China

[2]Institute of Atmospheric Physics, Chinese Academy of Sciences, Beijing 100029, China

[3]School of Chemistry, University of Leeds, Leeds LS2 9JT, UK

[4] Environment Research Institute, School of Environmental Science and Engineering, Shandong University, Ji'nan 250100, China

[5]The Beijing Innovation Center for Engineering Science and Advanced Technology, Peking University, Beijing, China

*Corresponding Author: tzhu@pku.edu.cn

Atmos. Chem. Phys. Discuss., doi:10.5194/acp-2016-410, 2016
Manuscript under review for journal Atmos. Chem. Phys.
Published: 24 May 2016

Atmospheric Chemistry and Physics Discussions

Abstract. The North China Plain (NCP) has been experiencing severe air pollution problems with rapid economic growth and urbanisation. Many field and model studies have examined the distribution of air pollutants in the NCP, but convincing results have not been achieved mainly due to a lack of direct measurements of pollutants over large areas. Here, we employed a mobile laboratory to observe the main air pollutants in a large part of the NCP from June 11 to July 15, 2013. High median concentrations of sulphur dioxide (SO_2) (12 ppb), nitrogen oxides (NO_x) ($NO+NO_2$; 452 ppb), carbon monoxide (CO) (956 ppb), black carbon (BC; 5.5 μg m^{-3}) and ultrafine particles (28350 cm^{-3}) were measured. Most of the high values, i.e., 95 percentile concentrations, were distributed near large cities, suggesting the influence of local emissions. In addition, we analysed the regional transport of SO_2 and CO, relatively long-lived pollutants, based on our mobile observations together with wind field and satellite data analyses. Our results suggested that, for border areas of the NCP, wind from outside would have a diluting effect on pollutants, while south winds would bring in pollutants accumulated during transport through other parts of the NCP. For the central NCP, the concentrations of pollutants were likely to remain at high levels, partly due to the influence of regional transport by prevalent south–north winds over the NCP and partly by local emissions.

Keywords: North China Plain, Air pollution, Distribution, On-road mobile measurements

Atmos. Chem. Phys. Discuss., doi:10.5194/acp-2016-410, 2016
Manuscript under review for journal Atmos. Chem. Phys.
Published: 24 May 2016

Atmospheric Chemistry and Physics Discussions

1. Introduction

The North China Plain (NCP) is a geographically flat region in the northern part of Eastern China, which includes Beijing, Tianjin, most of Hebei, Henan and Shandong provinces, and the northern parts of Anhui and Jiangsu provinces. This region is surrounded by the Yan Mountains to the north, the Taihang Mountains to the west and the Bohai Sea to the east. The NCP covers an area of 300,000 km^2, which corresponds to about 1/32 of the total area of China, but is home to approximately 1/5 of the Chinese population. The NCP is the political, economic and agricultural centre of China. Along with rapid economic growth and urbanisation, the NCP has been experiencing severe air pollution problems (Donkelaar et al., 2010). On a global scale, the NCP is a hotspot of nitrogen dioxide (NO_2), carbon monoxide (CO), sulphate and particulate matter (PM) concentrations, according to both satellite observations and model simulations (Chin et al., 1996; Yu et al., 2010; Bechle et al., 2011; Streets et al., 2013; Bucsela et al., 2013). The concentrations of PM with an aerodynamic diameter ≤ 2.5 μm ($PM_{2.5}$) and PM_{10} in the NCP are much higher compared to other rapidly developing areas in China, such as the Yangtze River Delta (Hu et al., 2014). According to the air-quality report published by the Chinese Ministry of Environmental Protection, in 2013, 9 of the 10 most polluted cities in China were located in the NCP. Severe pollution events occur frequently in this area. Therefore, studies of air pollution problems in the NCP are essential to obtain general insights into the unique patterns of air pollution in this area and for management of emissions control policies by the government.

Atmos. Chem. Phys. Discuss., doi:10.5194/acp-2016-410, 2016
Manuscript under review for journal Atmos. Chem. Phys.
Published: 24 May 2016

Atmospheric Chemistry and Physics Discussions

Over the past decade, there have been a number of investigations of air pollution in the NCP taking advantage of observation sites, aircraft measurement platforms, mobile laboratories, satellite data and air quality models. In the NCP, a network of observation sites has been built for air pollution research, mostly located in and around large cities, particularly Beijing (Xu et al., 2011; Xu et al., 2014; Wang et al., 2013; Meng et al., 2009; Shen et al., 2011; Lin et al., 2011). Variability, sources, meteorological and chemical impacts of air pollutants have been discussed by analysing these observational results. The concentrations of long-lived pollutants have been shown to be significantly influenced by wind, particularly the south and north winds, indicating that regional transport plays an important role in urban air pollution. In addition, model studies have yielded similar results in various areas of the NCP (An et al., 2007; Zhang et al., 2008; Liu et al., 2013). Satellite data have indicated that regional transport has a significant impact on the haze period in the NCP (Wang et al., 2014). Thus, it is necessary to understand regional transport to address air pollution problems in the NCP, which will require data on the distribution of air pollutants in this region.

However, observational data from a single or limited number of measurement sites cannot present the whole picture of air pollution in the NCP. A number of mobile laboratory measurements (Johansson et al. 2008; Li et al., 2009; Wang et al., 2009; Wang et al., 2011) and aircraft measurements (Huang et al. 2010; Zhang et al. 2011; Zhang et al. 2009; Zhang et al. 2014) have been used to determine pollution distributions mainly within the megacity of Beijing. There have been several reports

Atmos. Chem. Phys. Discuss., doi:10.5194/acp-2016-410, 2016
Manuscript under review for journal Atmos. Chem. Phys.
Published: 24 May 2016

Atmospheric Chemistry and Physics Discussions

of model and satellite studies on the air pollution distribution in the NCP, or even the whole of China (Wei et al., 2011; Zhao et al., 2013; Ying et al., 2014; Ding et al., 2015; Ding et al., 2009). However, there are disagreements between these results, e.g., regarding the distributions of NO_2 in several hotspot areas produced from model (CMAQ) and satellite (SCIAMACHY) measurements (Shi et al., 2008). Uncertainties in model simulations such as emissions inventories, and in satellite measurements such as the influence of clouds, can only be evaluated by measuring the spatial distributions of pollutants over a large geographical area, which are still lacking.

In this study, we measured the concentrations of nitrogen oxides (NO_x), CO, sulphur dioxide (SO_2), ultrafine particles and BC with a mobile laboratory platform in the NCP. Satellite data and field wind measurements during the observation period were also used. Our specific objectives were to collect a dataset showing the spatial distribution of air pollutants in the NCP, and to characterise the regional transport within and outside the NCP. This study was performed as part of the Campaigns of Air Pollution Research in Megacity Beijing and North China Plain (CAREBeijing-NCP 2013), and involved comprehensive stereoscopic observations, including observations of two super sites, several routine sites, mobile laboratories and model work. This paper focuses on the distribution and transport of pollutants in the NCP, mainly based on data collected from a mobile platform.

Atmos. Chem. Phys. Discuss., doi:10.5194/acp-2016-410, 2016
Manuscript under review for journal Atmos. Chem. Phys.
Published: 24 May 2016

Atmospheric Chemistry and Physics Discussions

2. Experimental methods

2.1 Mobile laboratory and study area

A mobile laboratory was built by our research group, details of which were previously described (Wang et al., 2009). Briefly, this mobile laboratory was constructed in 2006 on an IVECO Turin V diesel vehicle (L = 6.6 m, W = 2.4 m, H = 2.8 m; payload = 2.7 metric tonnes). Instrumentation was powered by two sets of uninterruptible power systems (UPS), consisting of three series of 48 V/110 Ah lithium batteries, which could support all of the equipment operations without interruption for up to 5 h. The inlet systems for our mobile laboratories were specifically configured to accommodate the type of measurement requirements and the instrument suite to be employed in specific field campaigns.

Instruments deployed on the mobile laboratory included those for studying NO_x, CO, SO_2, BC and ultrafine particles. NO_x was measured using an NO_x analyser with an Mo-converter (Ecotech model 9841A; Ecotech, Knoxfield, Melbourne, Australia), with a detection range of 0–500 ppb and uncertainty of 10 % at a time resolution of 30 s. CO was measured with a CO analyser by light absorption (Ecotech model 9830A) with a detection range of 0–9.8 ppm at a time resolution of 40 s. SO_2 was measured using an SO_2 analyser with a fluorescence cell (Ecotech model 9850A) with a detection range of 0–221.3 ppb at a time resolution of 120 s. BC was measured using a multi-angle absorption photometer (MAAP; Thermo model 5012; Thermo Scientific, Waltham, MA), with a detection range of 0–20 μg m^{-3}. The online measurement data

Atmos. Chem. Phys. Discuss., doi:10.5194/acp-2016-410, 2016
Manuscript under review for journal Atmos. Chem. Phys.
Published: 24 May 2016

Atmospheric Chemistry and Physics Discussions

from these instruments were recorded with an industrial personal computer.

Ultrafine particles were measured with a fast mobility particle sizer (FMPS, TSI 3090; TSI, Shoreview, MN), which covers particle sizes from 5.6 nm to 560 nm in 32 channels with a time resolution of 0.1 s. The data were recorded on a dedicated computer. Other auxiliary data including temperature, relative humidity, barometric pressure and GPS coordinates were also measured. The driving speed was kept stable at around 100 ± 5 km h^{-1} to cover as much distance as possible with the 5 h of power supplied by the lithium batteries.

To establish the spatial distribution and characterise the regional transport of air pollutants in the NCP, the routes for the mobile measurements were specially designed to cover important emissions hotspots (Fig. 1) and to map large areas of the NCP. The routes included the municipalities of Beijing and Tianjin, most of Hebei province, and part of Shandong province, which is about 300 km wide from the west to the east and 400 km long from the north to the south, covering most of the NCP. To avoid traffic jams and rough roads, only expressways were chosen for all routes. Limited by the duration of battery power and the variability of boundary layer height, we could not cover all routes in one trip. Instead, we divided the routes into five parts. Route 1 was along the Taihang Mountains from Beijing to Shijiazhuang, located in the western part of the NCP. Routes 2 and 3 were from Shijiazhuang to Dezhou and Cangzhou to Baoding, respectively, which were generally located in central NCP. Routes 4 and 5 were from Tianjin to Beijing and around the south of Beijing, located in northern NCP.

Atmos. Chem. Phys. Discuss., doi:10.5194/acp-2016-410, 2016
Manuscript under review for journal Atmos. Chem. Phys.
Published: 24 May 2016

Atmospheric Chemistry and Physics Discussions

144 In addition, we ran each route in one day. Two days were also needed for calibration
145 and maintenance of instruments. Therefore, it took one whole week to conduct a
146 single experiment. In total, six experiments, including one pre-test study, were
147 designed from June 1 to July 15, 2013. The pre-test study was conducted between
148 June 1 and June 7, and five formal repeated experiments were conducted between
149 June 11 and July 15 (Experiment 1 [E1], June 11–June 15; E2, June 17, June 18 and
150 June 20; E3, June 24–June 25; E4, July 2–July 7; E5, July 11–July 15). All trips were
151 started at about 09:00 and ended at about 14:00 to ensure that the boundary layer was
152 relatively stable during the observation period in 1 day. Unfortunately, data were
153 unavailable on several days because of heavy rain. The route design and trip runs are
154 shown in Figures 1 and 2, respectively.

155 Figure 1 here.

156 **2.2 The trajectories model**

157 A Lagrangian particle dispersion model, FLEXPART-WRF version 3.1 (Brioude et al.,
158 2013; Stohl et al., 1998; Stohl et al., 2005; Fast and Easter, 2006), was used to
159 determine the origin and transport pathways of the air mass arriving at the
160 vehicle-based mobile measurement laboratory. The wind field used to drive
161 FLEXPART was the time-averaged wind provided by the WRF with temporal
162 intervals of 10 min and horizontally spatial resolution of 2 km (The details of the
163 mesoscale meteorological model is described in S2.1). FLEXPART simulates the
164 transport and dispersion of tracers by calculating the backward trajectories of

Atmos. Chem. Phys. Discuss., doi:10.5194/acp-2016-410, 2016
Manuscript under review for journal Atmos. Chem. Phys.
Published: 24 May 2016

multitudinous particles, which are termed plume back trajectories. In this model, turbulence in the planetary boundary layer (PBL) is parameterised by solving the Langevin equation, and convection is parameterised using the Zivkovic Rothman scheme (Stohl et al., 2005). To improve the accuracy of the trajectory calculation, we used high-resolution WRF simulation domain 4 outputs as the input meteorological conditions for the FLEXPART model. The turbulence, convection and boundary layer height were computed along the trajectories of tracer particles using the WRF output data. Backward integration was performed every 5 min during the mobile observation period in June 2013. For each integration, 2000 stochastic particles were released initially from within a box 1 × 1 km^2 in horizontal extent and 1–50 m vertical height above ground centred on the mobile measurement laboratory. A total of 2000 inert tracer particles were released about every 5 min along the route of the vehicle. For each release, the backward trajectories were simulated for at least 12 h, and the particle locations were output every 10 min for analysis. The 12 h length of the backward trajectories was chosen as a trade-off to adequately sample the history of the air masses over the region of interest, while decreasing the trajectory error (Stohl, 1998; Zhang et al., 2012).

The footprints of backward trajectories were calculated to present plume trajectories. Footprints in this context refer to the total residence times of released particles, which were calculated following Ashbaugh et al. (1985) and de Foy et al. (2009) by counting the accumulated number of particles during the integration within each cell of a 2 × 2 km^2 grid. Various transport and diffusion patterns can well be

Atmos. Chem. Phys. Discuss., doi:10.5194/acp-2016-410, 2016
Manuscript under review for journal Atmos. Chem. Phys.
Published: 24 May 2016

described by these footprints analyses (Zhang et al., 2012).

2.3 Stationary measurement sites and the fire data

Concentrations of air pollutants, including NO_x, SO_2, CO and BC, were measured simultaneously at three stationary measurement sites during CAREBeijing-NCP 2013. These were rural sites located at Gucheng, Hebei province (GC, 39.13°N, 115.67°E), Quzhou, Hebei province (QZ, 36.78°N, 114.92°E) and Yucheng, Shandong province (YC, 36.67°N, 116. 37°E) (Fig. 1). The GC stationary site was near route 1, and QZ and YC stationary sites were near route 2.

The main pollutants at these sites were measured using commercial instruments. At the QZ site, gas analysers were used to measure NO_x (Ecotech model 9841A), CO (Ecotech model 9830A) and SO_2 (Ecotech model 9850A). At GC and YC stations, gas analysers were used to measure NO_x (Thermo model 42C), CO (Thermo model 48i) and SO_2 (Thermo model 48i), and BC was measured by MAAP (Thermo model 5012).

Fire data were obtained from the Moderate Resolution Imaging Spectroradiometer (MODIS) installed in Terra and Aura. The territory passing times were 10:30 (local time) and 13:30 (local time) for Terra and Aura, respectively. Fire images were obtained from EOSDIS Worldview (NASA, https://earthdata.nasa.gov/labs/worldview).

Atmos. Chem. Phys. Discuss., doi:10.5194/acp-2016-410, 2016
Manuscript under review for journal Atmos. Chem. Phys.
Published: 24 May 2016

Atmospheric Chemistry and Physics Discussions

3. Result and discussion

3.1 Distribution of air pollutants

BC, NO_x, CO and SO_2 were measured on five routes during the experiment to determine the concentrations of air pollutants on the routes and their spatial distributions in the NCP. Figure 2 shows the results of our mobile measurements obtained in 19 trips on the five routes from June 11 to July 15. The mean and median concentrations of BC, NO_x, CO and SO_2 were 5.8 and 5.5 μg m^{-3}, 422 and 452 ppb, 1006 and 956 ppb and 15 and 12 ppb, respectively, in the whole study. These high values were consistent with previous measurements of most pollutants at stationary measurement sites in the NCP except for NO_x. For example, the measured concentrations of NO_x, SO_2 and CO were 62.7 ± 4.0 ppb, 31.9 ± 2.0 ppb and 1990 ± 130 ppb in an urban site in the courtyard of China Meteorological Administration in the Beijing area from November 17, 2007, to March 15, 2008 (Lin et al., 2011). These values were 13–50 ppb, 5.7–30.3 ppb and 1100–1800 ppb at an urban site in Wuqing (between Beijing and Tianjin) from July 9, 2009, to January 21, 2010 (Wu et al., 2011); and 28.4 ppb, 17.2 ppb and 1520 ppb at the GC site from July 2006 to September 2007 (Lin et al., 2009). In addition, the concentration of NO_2 measured at the YC site from June 18 to June 30 was about 20 ppb (Wen et al., 2015). This comparison with stationary site measurements suggested that our mobile measurements reflected the heavily polluted conditions in the NCP, which ensured its feasibility in profiling the distributions of these air pollutants.

Atmos. Chem. Phys. Discuss., doi:10.5194/acp-2016-410, 2016
Manuscript under review for journal Atmos. Chem. Phys.
Published: 24 May 2016

Atmospheric Chemistry and Physics Discussions

227 Figure 2 here

228 The levels of CO, NO_x and BC here were also comparable to those in previous
229 mobile laboratory measurements in European and American cities. Bukowiecki et al.
230 (2002) measured CO in Zürich, Switzerland, and the average concentration was about
231 600 ppb. Hagemann et al. (2014) measured NO_x in Karlsruhe in Germany, and the
232 average concentration was about 20 ppb. In the USA, NO_x was around 50 ppb in
233 Somerville (Padró-Martínez 2012), 200 ppb during rush hour in Boston (Kolb et al.,
234 2004) and ranged from 230 ppb to 470 ppb in Los Angeles (Westerdahl et al., 2005).
235 Padró-Martínez et al. (2012) also measured BC in Somerville, and reported average
236 concentrations of about 1 μg m^{-3}. As these measurements were obtained in
237 heavy-traffic areas in large cities, and our results were measured over a large region,
238 we concluded that the air pollution problems in the NCP are among the worst in the
239 world.

240 In contrast to these pollutants, a low concentration of SO_2 was consistently
241 measured throughout the whole study. The low levels of SO_2 could be attributed to the
242 Chinese government's effort to install desulphurisation devices in power plants and
243 major industrial sources since 1996.

244 As shown in Figure 3, the concentrations of BC, NO_x, CO and SO_2 were highly
245 variable on the different routes in the NCP. The concentration ranges of these four
246 species were 5–14 μg m^{-3} for BC, 447–891 ppb for NO_x, 22.6–40.4 ppb for SO_2 and
247 1105–1652 ppb for CO. These extremely high values, i.e., 95 percentile

Atmos. Chem. Phys. Discuss., doi:10.5194/acp-2016-410, 2016
Manuscript under review for journal Atmos. Chem. Phys.
Published: 24 May 2016

248 concentrations, were consistently found in various plumes near these emissions
249 hotspots in the NCP, which suggested a major influence on concentrations of
250 measured species in these hotspot areas by local emissions. The hotspots observed
251 here were mainly around the junction areas of our design routes, and they included but
252 were not limited to areas of Beijing, Tianjin, Baoding, Cangzhou, Dezhou,
253 Shijiazhuang and Zhuozhou. Previous model simulations and satellite measurements
254 in the NCP also confirmed the high concentrations of NO_2 around these large cities
255 (Shi et al., 2008). It is worth noting that these observed concentration hotspots moved
256 around the emissions hotspots, probably as a result of the varied transport processes in
257 different trips. For example, a pollution plume was detected 100 km to the south of
258 Cangzhou on June 20, but 130 km to the north of Cangzhou on July 6. In addition,
259 plumes were not always detected in different experiments around these cities, with the
260 exception of Shijiazhuang.

261 Figure 3 here.

262 During the five experiments, no clear temporal distributions of air pollutant
263 concentrations in the NCP were seen, except for the significantly low levels of NO_x
264 and SO_2 observed in the last experiments. However, no connections between the
265 decline in NO_x and SO_2 concentrations and emissions or transport could be made. In
266 fact, the decline could probably be attributed to a wide range of precipitation that
267 occurred at that time.

268 In summary, our mobile laboratory measurements indicated spatial distributions of

Atmos. Chem. Phys. Discuss., doi:10.5194/acp-2016-410, 2016
Manuscript under review for journal Atmos. Chem. Phys.
Published: 24 May 2016

Atmospheric Chemistry and Physics Discussions

the pollutants SO_2, CO and BC and the number density of fine particles. The concentrations of air pollutants in the NCP were among the highest in the world and extremely high concentrations were also observed around several cities.

3.2 The influence of traffic emission

The levels and distributions of air pollutants in the NCP are mainly attributable to three sources, i.e., regional transport, local emissions and traffic emissions. On-road measurements, however, could be greatly affected by traffic emissions (Wang et al., 2009). The influence of traffic emissions on our mobile laboratory measurements is discussed below.

According to the emissions inventories, vehicles were a considerable source of NO_x, BC and CO. In the Beijing-Tianjin-Hebei area, the NO_x (Annual Report of Chinese Environmental Statistics [in Chinese], 2013), BC (Cao et al., 2006) and CO (Zhao et al., 2012) emissions from vehicles were 30.5 %, 2.4 % and 20 % of total emissions, respectively. SO_2 emissions from vehicles were negligible. Thus, the on-road measurements of NO_x, BC and CO would have been influenced by traffic emissions to various degrees. For example, mean and median values of NO_x concentration were 487 ± 213 ppb and 493 ppb in various routes in the first four experiments and 127 ± 100 ppb and 100 ppb even in the last experiment with the presence of wet deposition. These on-road values were much higher than those observed in the monitoring sites in surrounding cities. The mean NO_x concentrations were about 11 ± 6 ppb measured on June 11 at the GC site, 25 ± 10 ppb on June 12, 8.1 ± 0.91 ppb on June 18, 4.7 ± 1.2

Atmos. Chem. Phys. Discuss., doi:10.5194/acp-2016-410, 2016
Manuscript under review for journal Atmos. Chem. Phys.
Published: 24 May 2016

Atmospheric Chemistry and Physics Discussions

ppb on June 25, 6.3 ± 1.3 ppb on July 3, 3.2 ± 0.79 ppb on July 12 at the QZ site, and 13 ± 4.1 ppb on June 25 and 13 ± 1.8 ppb on July 3 at the YC site (Fig. 2).

In addition, a strong correlation (r^2 = 0.99) was found between on-road NO_x and NO (Fig. 4), with an average NO/NO_2 ratio of 4, which was much higher than the value of 0.05–0.2 in the aged plumes (Finlayson-Pitts and Pitts, 2010). The results indicated that NO_x observed by our mobile laboratory was mostly influenced by fresh vehicle emissions. Overall, the on-road NO_x observations here were not representative of the NO_x levels in the NCP.

Figure 4 here.

For BC, CO and SO_2, the concentrations measured by the mobile laboratory and nearby monitoring sites were comparable to some extent (Fig. 2). The BC concentrations measured in nearby monitoring sites were 2.8 ± 1.4 μg m^{-3} (June 12, QZ), 4.9 ± 0.72 μg m^{-3} (June 18, QZ) and 4.9 ± 1.1 μg m^{-3} (June 25, YC). Compared to stationary measurements, the BC concentrations measured by the mobile laboratory were slightly higher, 4.8 ± 2.2 μg m^{-3} on June 12, 6.8 ± 2.3 μg m^{-3} on June 18 and 6.5 ± 3.3 μg m^{-3} on June 25. The CO concentrations measured at monitoring sites were 1220 ± 910 ppb (June 12, QZ), 1000 ±140 ppb (June 18, QZ), 730 ± 210 ppb (June 25, YC) and 520 ± 190 ppb (July 3, YC). Similarly, the CO concentrations measured by the mobile laboratory were 950 ± 440 ppb on June 12, 1030 ± 530 ppb on June 18, 1020 ± 680 ppb on June 25 and 990 ± 450 ppb on July 3. The SO_2 concentrations measured at monitoring sites were 10 ± 2.4 ppb (June 11, GC), 3.4 ± 0.57 ppb (July 11,

Atmos. Chem. Phys. Discuss., doi:10.5194/acp-2016-410, 2016
Manuscript under review for journal Atmos. Chem. Phys.
Published: 24 May 2016

Atmospheric Chemistry and Physics Discussions

311 GC), 30 ± 20 ppb (June 12, QZ), 12 ± 4.2 ppb (June 25, QZ) and 10 ± 4.6 ppb (June
312 25, YC). Meanwhile, the SO_2 concentrations measured by the mobile laboratory were
313 higher in some trips and lower in others compared to the stationary measurements.
314 For example, lower SO_2 concentrations of 6.6 ± 5.5 ppb on June 11 and of 26 ± 11
315 ppb on June 12 were measured in these two trips, and higher SO_2 concentrations of
316 7.1 ± 2.9 ppb on July 11 and of 27 ± 16 ppb on June 25 in other trips. In addition, the
317 concentrations of BC, CO and SO_2 were not correlated with those of NO. Traffic is
318 not a major source of atmospheric CO over the NCP region, as determined by
319 comparing CO column concentration from the satellite and traffic flux (Wu et al.,
320 2011).

321 Thus, unlike NO_x, gas pollutants including BC, CO and SO_2 were mainly affected
322 by sources, such as local emissions and transport, other than traffic emissions. The
323 mobile laboratory observations reported here could accurately reflect the
324 concentrations and spatial distributions of BC, CO and SO_2 in the NCP.

325 **3.3 The influence of regional transport**

326 Local emissions and regional transport are the two main sources of pollutants in the
327 NCP (Xu et al., 2011). As stated above, local emissions in large cities had a major
328 impact on the air quality in their adjacent areas. Regional transport also plays a major
329 role. Our study demonstrated that the contribution of regional transport could vary
330 both spatially and temporally, depending on a number of parameters, such as
331 prevalent wind, terrain and vertical mixing. We also roughly divided the NCP into two

Atmos. Chem. Phys. Discuss., doi:10.5194/acp-2016-410, 2016
Manuscript under review for journal Atmos. Chem. Phys.
Published: 24 May 2016

Atmospheric Chemistry and Physics Discussions

parts according to these parameters, i.e., the northern border area and the central area, to discuss the influence of regional transport on air quality.

3.3.1 The border areas of NCP

The northern border area of the NCP included major parts of routes 4 and 5 and the western border areas of the NCP included a major part of route 1. The area is surrounded by the Taihang Mountains to the west and the Yan Mountains to the north. The north wind prevailed in the winter and the south wind prevailed in the summer in this area.

During the measurements, the three routes experienced both north and south winds. Specifically, northwest winds and east winds brought outside air masses from Northeast China and the Bohai Sea to the northern border area on July 2 and July 7, respectively (Fig. 5). In both trips, the concentrations of SO_2, CO and BC were 4.5 ± 2.3 ppb, 550 ± 240 ppb and 5.0 ± 2.6 μg m^{-3}, respectively, on July 2 and 7.0 ± 3.0 ppb, 1090 ± 320 ppb and 6.5 ± 2.7 μg m^{-3}, respectively, on July 7 (Fig. 2), which were the lowest values observed here in the border areas of the NCP. These observations were reasonable as areas including the Bohai Sea to the west, north and east of the NCP were regions of low emissions and the clean air brought by northeast and east winds could dilute the air pollutants in the border areas of the NCP.

Figure 5 here.

It is worth noting that the BC concentration was not lowest on July 2, which was

Atmos. Chem. Phys. Discuss., doi:10.5194/acp-2016-410, 2016
Manuscript under review for journal Atmos. Chem. Phys.
Published: 24 May 2016

Atmospheric Chemistry and Physics Discussions

the opposite of the observations for the gas pollutants, SO_2 and CO. Satellite images showed that there were many fire plots near route 1 on July 2 (Fig. S2). A featured single peak of aerosol number density at around 50 nm (Fig. S3) further confirmed that BC emissions from agricultural crop residue burning contributed significantly to the BC levels on July 2 (Zhang et al., 2011; Hays et al., 2005; Li et al., 2007).

On June 24, June 14 and June 15, the air masses were transported inside the NCP from the southern NCP to the northern border areas by south winds (Fig. 5). Under these wind conditions, the concentrations of SO_2, CO and BC were 15 ± 5.8 ppb, 1300 ± 330 ppb and 8.0 ± 1.4 μg m^{-3}, respectively, on June 24, 26 ± 7.9 ppb, 1200 ± 230 ppb and 6.5 ± 1.5 μg m^{-3}, respectively, on June 14 and 28 ± 7.1 ppb, 1600 ± 370 ppb and 7.0 ± 1.9 μg m^{-3}, respectively, on June 15 (Fig. 2), which were among the highest levels detected on these routes. According to the emissions inventories (Fig. 3), most emissions hotspots were located in the central and southern parts of the NCP. Pollutants could be easily accumulated in air masses of south and central NCP origin. In addition, the Yan Mountains to the north of the border area stopped the possible transport pathway of these air masses, which further enhanced the accumulation of long-lived air pollutants in the northern border area of the NCP.

Although route 4 on July 6 was under the influence of south winds, as on June 14 (Fig. 5), the concentrations of SO_2 and BC on July 6 were 14 ± 7.6 ppb and 4.6 ± 1.8 μg m^{-3}, respectively, on July 6, which were much lower than the values of 26 ± 7.9 ppb and 6.5 ± 1.5 μg m^{-3}, respectively, on June 14. Meanwhile, the CO levels on these

Atmos. Chem. Phys. Discuss., doi:10.5194/acp-2016-410, 2016
Manuscript under review for journal Atmos. Chem. Phys.
Published: 24 May 2016

two days were similar. One possible cause of the low concentrations of both SO_2 and BC was the slightly higher boundary layer height on July 6 compared to June 14. The precipitation that occurred on July 6, but not on June 14, appeared to be a more important contributing factor. The solubility of CO is less than that of SO_2. Therefore, the wet deposition lifetime of SO_2 would be much shorter, thus limiting the transport distance of SO_2. Meanwhile, the wet deposition of BC particles would also prohibit its long-range transport. This may explain the similar CO levels and low SO_2 and BC levels on July 6 at the same time.

In conclusion, for the northern border area, local emissions and regional transport from other NCP areas due to south winds were two main sources of long-lived pollutants; both north and east winds had significant dilution effects on the concentrations of gas pollutants. The wind dependency scatter plots for SO_2 were used to show the contribution of regional transport to air pollution in the northern border area of the NCP (Fig. 6). The results indicated that the high concentration was connected to the south wind at a wind speed from 4 to 10 m s^{-1}. Similar results for SO_2 and CO were reported for several sites in the northern NCP (Wu et al., 2011; Lin et al., 2011; Lin et al., 2009). As the south wind usually prevailed in the summer and north wind in the winter, the regional transport of long-lived pollutants within the NCP from the central and southern parts to the northern parts should be prevalent in the summer; while the dilution of air pollutants mainly by north winds and occasionally east winds should be prevalent for the northern parts of the NCP in the winter.

Atmos. Chem. Phys. Discuss., doi:10.5194/acp-2016-410, 2016
Manuscript under review for journal Atmos. Chem. Phys.
Published: 24 May 2016

Atmospheric Chemistry and Physics Discussions

395 Figure 6 here.

396 **3.2.2 The central NCP**

397 The central NCP consisted of routes 2 and 3, where numerous heavily polluted cities
398 are located. The area was surrounded by the Taihang Mountains to the west or
399 emissions hotspots in other directions. While the north wind prevailed in the winter, as
400 for the northern border areas, low pressure prevailed in the summer with south and
401 northeast winds in this area.

402 During the observation period, the measurements along the two routes experienced
403 different wind fields, including southwest winds on June 12 and July 3, northeast
404 winds on June 18 and a low-pressure system with south and northeast winds on June
405 25 (Fig. S4). Unlike the northern border area of the NCP where strong north winds
406 had a dilution effect, the concentrations of gas pollutants were mostly high regardless
407 of the wind direction in the central NCP, e.g., on June 18 and July 3 (Fig. S4).
408 Generally, our observations were reasonable according to the unique terrain and
409 emissions map in central NCP. Due to the heavy emissions level in the central NCP
410 and surrounding areas, pollutants readily accumulated to high levels on their ways to
411 the central NCP in air masses from all directions, such as the clean air masses from
412 the Bohai Sea, West China and Northeast China, and polluted air masses from
413 Southeast China.

414 The situation was slightly different in areas along route 3, particularly for those off

Atmos. Chem. Phys. Discuss., doi:10.5194/acp-2016-410, 2016
Manuscript under review for journal Atmos. Chem. Phys.
Published: 24 May 2016

415 the coast of the Bohai Sea. Route 3 experienced east winds on July 14 (Fig. S4), and
416 the concentrations of pollutants were low (Fig. 2). This was not only because of the
417 wet deposition from the rain on that day, but also the transport of clean air from the
418 Bohai Sea. A featured peak of aerosol number density at around 20 nm (Fig. S3)
419 further confirmed the incoming air from the Bohai Sea (Haaf and Jaenicke, 1980;
420 Hoppel et al., 1986).

421 Vertical mixing can also affect the concentrations of pollutants. For example, while
422 the wind fields were similar on June 13 and July 4 (Fig. 7), the concentration of
423 pollutants on June 13 was lower than that on July 4 (Fig. 2). This was because the
424 boundary layer was much higher on June 13 (976 m) than on July 4 (626 m), and the
425 strong vertical convection diluted the air pollutants.

426 Specifically, the relative contributions of emissions and regional transport to the
427 local air pollution levels were slightly different on different routes. At the junction of
428 routes 1 and 2 around Shijiazhuang area, the concentrations of air pollutants were
429 always high, except in the last experiment when wet precipitation occurred. The local
430 emissions contributed significantly to the air pollution levels in this area. The city of
431 Shijiazhuang is known as an emissions hotspot with heavy coal consumption.
432 Previous model result showed that Shijiazhuang is an important emissions hotspot of
433 SO_2 even in the whole NCP area (He et al., 2012). Meanwhile, the Taihang Mountains
434 to the west of the city prevented the diffusion of air pollutants. On the other hand,
435 transport convergence in front of the Taihang Mountains and Yan Mountains was

Atmos. Chem. Phys. Discuss., doi:10.5194/acp-2016-410, 2016
Manuscript under review for journal Atmos. Chem. Phys.
Published: 24 May 2016

Atmospheric Chemistry and Physics Discussions

436 proposed in a previous study (Su et al., 2004), as a result of a low-pressure system
437 along the Taihang Mountains and Yan Mountains. Although the transport convergence
438 moved around in the north end, it always passed by the Shijiazhuang area. As shown
439 in Figure 3, high levels of pollutants, particularly relatively long-lived species such as
440 SO_2 and CO, were consistently observed at the western end of route 2 near
441 Shijiazhuang area. Broad peaks of SO_2 and CO concentrations, indicators of regional
442 transport plumes, were present near Shijiazhuang area (Fig. S5).

443 Similar to the situation in Shijiazhuang area, transport convergence would
444 occasionally pass through other cities along routes 2 and 3. In a typical case on June
445 13 (Fig. 7), air masses were transported far from the southwest of the NCP along the
446 transport convergence through Shijiazhuang and reached the area on route 3, with air
447 pollutants accumulating during transport and showing high concentrations.

448 Figure 7 here.

449 Overall, in most areas in central NCP, regional transport would play essential soles
450 in determining the local air pollution levels, although the underlying mechanisms
451 were different for the transport convergence area, central NCP area and coastal area.
452 The wind dependence scatter plots for SO_2 and CO were used as examples to show
453 the contribution of regional transport on air pollution in central NCP (Fig. 6). The
454 results indicated that the prevailing winds were southwest and northeast in central
455 NCP during our observation period. The concentrations of CO were independent of
456 wind direction and wind speed. In addition, the high concentrations of SO_2 were

Atmos. Chem. Phys. Discuss., doi:10.5194/acp-2016-410, 2016
Manuscript under review for journal Atmos. Chem. Phys.
Published: 24 May 2016

Atmospheric Chemistry and Physics Discussions

related to southeast winds with high speed, which was about 5–10 m s^{-1}. This may have been because of transport convergence. Due to the strong interaction of different areas in central NCP, emissions control policies must consider the whole emissions budget to achieve the air quality aims.

4. Conclusion

A mobile laboratory was employed to obtain snapshots of the spatial distributions of air pollutants in the NCP. The concentrations observed were at the highest levels in the world and were distributed unevenly in the NCP. Most high concentrations, i.e., 95 percentile concentrations, of air pollutants were found near emissions hotspots, which suggested the influence of local emissions. However, regional transport of air pollutants was also considered significant in determining the air quality in the NCP. Back trajectory analysis, satellite data and tracer pollutants were combined to recognise various cases of regional transport in both the northern border and central NCP. Where the border areas would occasionally be diluted by winds from outside the NCP, the central NCP was affected by regional transport of air pollutants with a few exceptions, such as when precipitation occurred. To achieve the aims of air quality locally, emissions control policies must consider the whole emissions budget in the NCP.

The English in this document has been checked by at least two professional editors, both native speakers of English. For a certificate, please see:

http://www.textcheck.com/certificate/bENNRx

Data availability. The data of mobile and stationary measurements are available upon requests.

Author contribution. T. Zhu, Y. Zhu, Y. Han and W. Chen designed the experiments. T. Zhu secured the research grants. Y. Zhu, Y. Han and W. Chen carried out the experiments. J. Zhang developed the model code and performed the simulations. J. Wang managed the data in the program. J. Liu provided the emission maps. L. Zeng, Y. Wu, X. Wang, W. Wang and J. Chen provided the data of stationary measurements. Y. Zhu analyzed the data with contributions from all co-authors. Y. Zhu prepared the manuscript with helps from T. Zhu, C. Ye and Y. Li.

Acknowledgement. This study was supported by the National Natural Science Foundation Committee of China (21190051, 41121004, 41421064), the European 7th Framework Programme Project PURGE (265325), the Collaborative Innovation Center for Regional Environmental Quality.

5. References

An, X., Zhu, T., Wang, Z., Li, C., and Wang, Y.: A modeling analysis of a heavy air pollution episode occurred in Beijing, Atmos. Chem. Phys., 7, 3103–3114, 2007.

496 Ashbaugh, L. L., Malm, W. C., and Sadeh, W. Z.: A residence time probability
497 analysis of sulfur concentrations at Grand Canyon National Park, Atmos. Environ.,
498 19, 1263–1270, 1985.

499 Bechle, M. J., Millet, D. B., and Marshall, J. D.: Effects of income and urban form on
500 urban NO_2: Global evidence from satellites, Environ. Sci. Technol., 45, 4914–4919,
501 doi: 10.1021/es103866b, 2011.

502 Brioude, J., Arnold, D., Stohl, A., Cassiani, M., Morton, D., Seibert, P., Angevine, W.,
503 Evan, S., Dingwell, A., Fast, J., Easter, R., Pisso, I., Burkhart, J. and Wotawa, G.:
504 The Lagrangian particle dispersion model FLEXPART-WRF version 3.1,
505 Geoscientific Model Development, 6, 1889-1904, doi:10.5194/gmd-6-1889-2013,
506 2013.

507 Bucsela, E. J., Krotkov, N. A., Celarier, E. A., Lamsal, L. N., Swartz, W. H., Bhartia,
508 P. K., Boersma, K. F., Veefkind, J. P., Gleason, J. F., and Pickering, K. E.: A new
509 stratospheric and tropospheric NO_2 retrieval algorithm for nadir-viewing satellite
510 instruments: applications to OMI, Atmos. Meas. Tech., 6, 2607–2626, doi:
511 10.5194/amtd-6-1361-2013, 2013.

512 Bukowiecki, N., Dommen, J., Prévôt, A. S. H., Richter, R., Weingartner, E., and
513 Baltensperger, U.: A mobile pollutant measurement laboratory-measuring gas
514 phase and aerosol ambient concentrations with high spatial and temporal resolution,
515 Atmos. Environ., 36, 5569-5579, 2002.

516 Cao, G., Zhang, X., Wang, Y., Che, H., and Chen, D.: Inventory of black carbon
517 emission from China, Adv. Clim. Change Res., 3, 75-81, 2007.

518 Cao, G., Zhang, X., and Zheng, F.: Inventory of black carbon and organic carbon
519 emissions from China, Atmos. Environ., 40, 6516-6527, 2006.

520 Chin, M., and Jacob, D. J.: Anthropogenic and natural contributions to tropospheric
521 sulfate: A global model analysis, J. Geophys. Res., 101, 18691-18699, doi:
522 10.1029/96JD01222, 1996.

523 de Foy, B., Zavala, M., Bei, N., and Molina, L.: Evaluation of WRF mesoscale
524 simulations and particle trajectory analysis for the MILAGRO field campaign,
525 Atmos. Chem. Phys, 9, 4419-4438, 2009.

526 Ding, A., Wang, T., Xue, L., Gao, J., Stohl, A., Lei, H. C., Jin, D. Z., Ren, Y., Wang,
527 X. Z., Wei, X. L., Qi, Y. B., Liu, J., and Zhang, X. Q.: Transport of north China air
528 pollution by midlatitude cyclones: Case study of aircraft measurements in summer
529 2007, J. Geophys. Res., 114, D11399, doi:10.1029/2009JD012339, 2009.

530 Ding, K., Liu, J., Ding, A., Liu, Q., Zhao, T., Shi, J., Han, Y., Wang, H., and Jiang, F.:
531 Uplifting of carbon monoxide from biomass burning and anthropogenic sources to
532 the free troposphere in East Asia, Atmos. Chem. Phys., 15, 2843–2866, 2015.

533 Donkelaar, V. A., Martin, R. V., Brauer, M., Kahn, R., Levy, R., Verduzco, C., and
534 Villeneuve, P. J.: Global estimates of ambient Fine particulate matter concentrations

535 from satellite-based aerosol optical depth: development and application, Environ.
536 Health Perspect., 118, 847-855, doi: 10.1289/ehp.0901623, 2010.

537 Fast, J. D. and Easter, R. C.: A Lagrangian particle dispersion model compatible with
538 WRF, in: 7th WRF User's Workshop, NCAR, P6-02, 19–22 June, Boulder,
539 Colorado, 2006.

540 Finlayson-Pitts, B. J. and Pitts, J. N.: Chemistry of the upper and lower atmosphere,
541 Academic press, San Diego, California, USA, 2010.

542 Haaf, W., and Jaenicke, R.: Results of improved size distribution measurements in the
543 Aitken range of atmospheric aerosols, J. Aerosol Sci., 11, 321–330, doi:
544 10.1016/0021-8502(80)90106-8, 1980.

545 Hagemann, R., Corsmeier, U., Kottmeier, C., Rinke, R., Wieser, A., and Vogel, B.:
546 Spatial variability of particle number concentrations and NOx in the Karlsruhe
547 (Germany) area obtained with the mobile laboratory 'AERO-TRAM', Atmos.
548 Environ., 94, 341-352, doi: 10.1016/j.atmosenv.2014.05.051, 2014.

549 He, H., Li, C., Loughner, C. P., Li, Z., Krotkov, N. A., Yang, K., Wang, L., Zheng, Y.,
550 Bao, X., Zhao, G., and Dickerson, R. R.: SO_2 over central China: Measurements,
551 numerical simulations and the tropospheric sulfur budget, J. Geophys. Res., 117,
552 D00K37, doi: 10.1029/2011JD016473, 2012.

553 Hoppel, W. A., Frick, G. M., and Larson, R. E.: Effect of nonprecipitating clouds on
554 the aerosol size distribution in the marine boundary layer, Geophys. Res. Lett., 13,

555 125–128, doi: 10.1029/GL013i002p00125, 1986.

556 Hu J., Wang Y., Ying Q., and Zhang H.: Spatial and temporal variability of $PM_{2.5}$ and
557 PM_{10} over the North China Plain and the Yangtze River Delta, China, Atmos.
558 Environ., 95, 598-609, 2014.

559 Huang, K., Zhuang, G., Lin, Y., Li, J., Sun, Y., Zhang, W., and Fu, S.: Relation
560 between optical and chemical properties of dust aerosol over Beijing, China, J.
561 Geophys. Res., 115, doi: 10.1029/2009JD013212, 2010.

562 Johansson, M., Galle, B., Yu, T., Tang, L., Chen, D., Li, H., Li, J., and Zhang, Y.:
563 Quantification of total emission of air pollutants from beijing using mobile
564 mini-doas, Atmos. Environ., 42, 6926–6933, doi: 10.1016/j.atmosenv.2008.05.025,
565 2008.

566 Kolb, C., Herndon, S., Mcmanus, J. B., Shorter, J., Zahniser, M., Nelson, D., and
567 Jayne, J., Canagaratna, M. R., and Worsnop, D. R.: Mobile laboratory with rapid
568 response instruments for real-time measurements of urban and regional trace gas
569 and particulate distributions and emission source characteristics, Environ. Sci.
570 Technol. 38, 5694-5703, doi: 10.1021/es030718p, 2004.

571 Li, A., Xie, P., Liu, W., Liu, J., and Dou, K.: Studies on the determination of the flux
572 of gaseous pollutant from an area by passive differential optical absorption
573 spectroscopy, (in Chinese), Spectrosc. Spect. Analys., 29, 28–32, doi:
574 10.3964/j.issn.1000-0593(2009)01-0028-05, 2009.

575 Lin, W., Xu, X., Ge, B., and Liu, X.: Gaseous pollutants in Beijing urban area during
576 the heating period 2007–2008: variability, sources, meteorological, and chemical
577 impacts, Atmos. Chem. Phys., 11, 8157–8170, 2011.

578 Lin, W., Xu, X., Ge, B., and Zhang, X.: Characteristics of gaseous pollutants at
579 Gucheng, a rural site southwest of Beijing, J. Geophys. Res., 114, doi:
580 10.1029/2008JD010339, 2009.

581 Liu, X., Li, J., Qu, Y., Han, T., Hou, L., Gu, J., Chen, C., Yang, Y., Liu, X., Yang, T.,
582 Zhang, Y., Tian, H., and Hu, M.: Formation and evolution mechanism of regional
583 haze: a case study in the megacity Beijing, China, Atmos. Chem. Phys., 13,
584 4501-4514, 2013.

585 Meng, Z., Xu, X., Yan, P., Ding, G., Tang, J., Lin, W., Xu, X., and Wang, S.:
586 Characteristics of trace gaseous pollutants at a regional background station in
587 Northern China, Atmos. Chem. Phys., 9, 927–936, 2009.

588 Padró-Martínez, L. T., Patton, A. P., Trull, J. B., Zamore, W., Brugge, D., and Durant,
589 J. L.: Mobile monitoring of particle number concentration and other traffic-related
590 air pollutants in a near-highway neighborhood over the course of a year, Atmos.
591 Environ., 61, 253-264, 2012.

592 Peters, J., Theunis, J., Poppel, M. V., and Berghmans, P.: Monitoring PM_{10} and
593 Ultrafine Particles in Urban Environments Using Mobile Measurements, Aerosol
594 Air Qual. Res., 13, 509–522, doi: 10.4209/aaqr.2012.06.0152, 2013.

595 Qu, L., Li, M., Chen, D., Lu, K., Jin, T., and Xu. X.: Multivariate analysis between
596 driving condition and vehicle emission for light duty gasoline vehicles during rush
597 hours, Atmos. Environ., 110, 103-110, 2015.

598 Shen, X., Yao, Z., Zhang, Q., Wagner, D. V., Huo, H., Zhang, Y., Zheng, B., and He,
599 K.: Development of database of real-world diesel vehicle emission factors for
600 China, J. Environ. Sci., 31, 209–220, doi: 10.1016/j.jes.2014.10.021, 2015.

601 Shen, X., Sun, J., Zhang, Y., Wehner, B., Nowak, A., Tuch, T., Zhang, X., Wang, T.,
602 Zhou, H., Zhang, X., Dong, F., Birmili, W., and Wiedensohler, A.: First long-term
603 study of particle number size distributions and new particle formation events of
604 regional aerosol in the North China Plain, Atmos. Chem. Phys., 11, 1565–1580,
605 2011.

606 Shi, C., Fernand, H. J. S., Wang, Z., An, X., and Wu, Q.: Tropospheric NO_2 columns
607 over East Central China: Comparisons between SCIAMACHY measurements and
608 nested CMAQ simulations, Atmos. Environ., 42, 7165–7173, 2008.

609 Stohl, A., Forster, C., Frank, A., Seibert, P., and Wotawa, G.: Technical note: The
610 Lagrangian particle dispersion model FLEXPART version 6.2, Atmos. Chem. Phys.,
611 5, 2461–2474, 2005.

612 Stohl, A.: Computation, accuracy and applications of trajectories – A review and
613 bibliography, Atmos. Environ., 32, 947–966, 1998.

614 Streets, D. G., Canty, T., Carmichael, G. R., Foy, B. D., Dickerson, R. R., Duncan, B.
615 N., Edwards, D. P., Haynes, J. A., Henze, D. K., Houyoux, M. R., Jacob, D. J.,
616 Krotkov, N. A., Lamsal, L. N., Liu, Y., Lu, Z. F., Martin, R. V., Pfister, G. G.,
617 Pinderm, R. W., Salawitch, R. J., and Wecht, K. J.: Emissions estimation from
618 satellite retrievals: A review of current capability, Atmos. Environ., 77, 1011-1042,
619 2013.

620 Su, F., Ren Z., Gao, Q., and Zhang Z.: Convergence System of Air Contamination in
621 Boundary Layer above Beijing and North China: Transport Convergence in
622 Boundary Layer, Res. Environ. Sci., 17, 21-25, doi：10.13198/j.res.2004.01.23.sufq.
623 004, 2004.

624 Wang Y., Yao L., Wang L., Liu Z., Ji D., Tang G., Zhang J., Sun Y., Hu B., and Xin
625 J.: Mechanism for the formation of the January 2013 heavy haze pollution episode
626 over central and eastern China, Sci. China (Earth Sci.), 57, 14-25, doi:
627 10.1007/s11430-013-4773-4, 2014.

628 Wang, M., Zhu, T., Zhang, J., Zhang, Q., Lin, W., Li, Y., and Wang, Z.: Using a
629 mobile laboratory to characterize the distribution and transport of sulfur dioxide in
630 and around Beijing, Atmos. Chem. Phys., 11, 11631–11645, 2011.

631 Wang, M., Zhu, T., Zheng, J., Zhang, R., Zhang, S., Xie, X., Han, Y., and Li, Y.: Use
632 of a mobile laboratory to evaluate changes in on-road air pollutants during the
633 Beijing 2008 Summer Olympics, Atmos. Chem. Phys., 9, 8247–8263, 2009.

634 Wang, X., Westerdahl, D., Hu, J., Wu, Y., Yin, H., Pan, X., and Zhang, K.: On-road
635 diesel vehicle emission factors for nitrogen oxides and black carbon in two Chinese
636 cities, Atmos. Environ., 46, 45-55, 2012.

637 Wang, X., Westerdahl, D., Wu, Y., Pan, X., and Zhang, K.: On-road emission factor
638 distributions of individual diesel vehicles in and around Beijing, China, Atmos.
639 Environ., 45, 503-513, 2011.

640 Wang, Z., Hu, M., Sun, J., Wu, Z., Yue, D., Shen, X., Zhang, Y., Pei, X., Cheng, Y.,
641 and Wiedensohler, A.: Characteristics of regional new particle formation in urban
642 and regional background environments in the North China Plain, Atmos. Chem.
643 Phys., 13, 12495–12506, 2013.

644 Wei, P., Cheng, S., Li, J., and Su, F.: Impact of boundary-layer anticyclonic weather
645 system on regional air quality, Atmos. Environ., 45, 2453-2463, 2011.

646 Westerdahl, D., Fruin, S., Sax, T., Fine, P., and Sioutas, C.: Mobile platform
647 measurements of ultrafine particles and associated pollutant concentrations on
648 freeways and residential streets in Los Angeles, Atmos. Environ., 39, 3597-3610,
649 2005.

650 Westerdahl, D., Wang, X., Pan, X., and Zhang, K.: Characterization of on-road
651 vehicle emission factors and microenvironmental air quality in Beijing, China,
652 Atmos. Environ., 43, 697-705, 2009.

653 Xu, W., Zhao, C., Ran, L., Deng, Z., Liu, P., Ma, N., Lin, W., Xu, X., Yan, P., He, X.,
654 Yu, J., Liang, W., and Chen, L.: Characteristics of pollutants and their correlation
655 to meteorological conditions at a suburban site in the North China Plain, Atmos.
656 Chem. Phys., 11, 4353–4369, 2011.

657 Xu, W., Zhao, C., Ran, L., Lin, W., Yan, P., and Xu, X.: SO_2 noontime-peak
658 phenomenon in the North China Plain, Atmos. Chem. Phys., 14, 7757–7768, 2014.

659 Yao, X., Lau, N. T., Fang, M., and Chan, C.: Real-time observation of the
660 transformation of ultrafine atmospheric particle modes, Aerosol Sci. Tech., 39,
661 831-841, doi: 10.1080/02786820500295248, 2005.

662 Ying, Q., Wu, L., and Zhang, H.: Local and inter-regional contributions to $PM_{2.5}$
663 nitrate and sulfate in China, Atmos. Environ., 94, 582-592, 2014.

664 Yu, F., Luo, G., Bates, T. S., Anderson, B., Clarke, A., Kapustin, V., Yantosca, R. M.,
665 Wang, Y., and Wu, S.: Spatial distributions of particle number concentrations in the
666 global troposphere: Simulations, observations, and implications for nucleation
667 mechanisms, J. Geophys. Res., 115, D17205, doi: 10.1029/2009JD013473, 2010.

668 Zhang, J., Zhu, T., Zhang, Q., Li, C., Shu, H., Ying, Y., Dai, Z., Wang, X., Liu, X.,
669 Liang, A., Shen, H. and Yi, B.: The impact of circulation patterns on regional
670 transport pathways and air quality over Beijing and its surroundings, Atmos. Chem.
671 Phys., 12, 5031-5053, 2012.

672 Zhang, Q., Ma, X., Tie, X., Huang, M., Zhao, C.: Vertical distributions of aerosols
673 under different weather conditions: Analysis of in-situ aircraft measurements in
674 Beijing, China, Atmos. Environ., 43, 5526–5535, 2009.

675 Zhang, Q., Quan, J., Tie, X., Huang, M., and Ma, X.: Impact of aerosol particles on
676 cloud formation: Aircraft measurements in China, Atmos. Environ., 45, 665-672,
677 2011.

678 Zhang, W., Zhu, T., Yang, W., Bai, Z., Sun, Y., Xu, Y., Yin, B., and Zhao, X.:
679 Airborne measurements of gas and particle pollutants during CAREBeijing-2008,
680 Atmos. Chem. Phys., 14, 301–316, 2014.

681 Zhang, Y., Hua, M., Zhong, L., Wiedensohler, A., Liu, S., Andreae, M. O., Wang, W.,
682 Fan, S.: Regional Integrated Experiments on Air Quality over Pearl River Delta
683 2004 (PRIDE-PRD2004): Overview, Atmos. Environ., 42, 6157–6173, 2008.

684 Zhao, B., Wang, S., Wang, J., Fu, J., Liu, T., Xu, J., Fu, X., and Hao, J.: Impact of
685 national NO_x and SO_2 control policies on particulate matter pollution in China,
686 Atmos. Environ., 77, 453-463, 2013.

687 Zhao, Y., Nielsen, C. P., McElroy, M. B., Zhang, L. and Zhang, J.: CO emissions in
688 China: Uncertainties and implications of improved energy efficiency and emission
689 control, Atmos. Environ., 49, 103-113, 2012.

Atmos. Chem. Phys. Discuss., doi:10.5194/acp-2016-410, 2016
Manuscript under review for journal Atmos. Chem. Phys.
Published: 24 May 2016

Atmospheric Chemistry and Physics Discussions

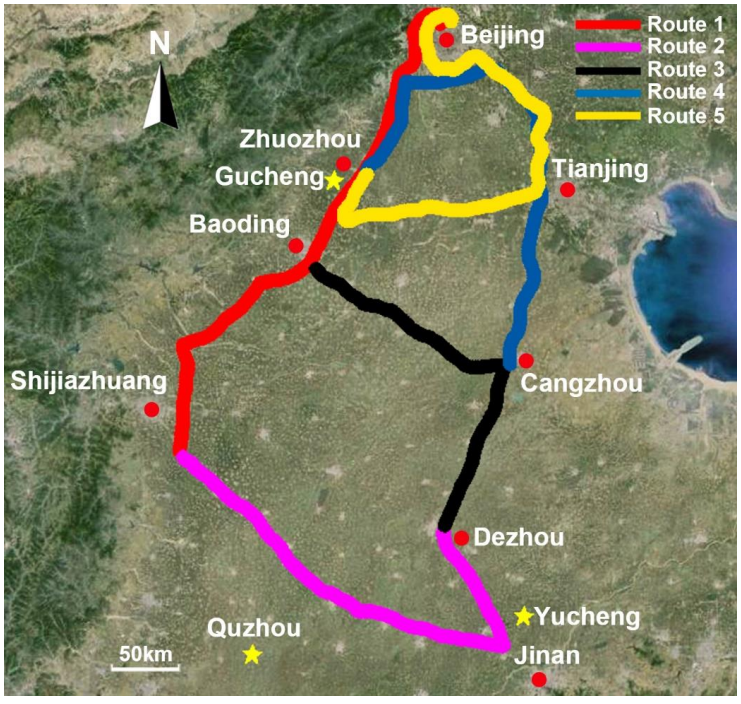

690

691 **Fig. 1.** The study area in NCP. The red track shows route 1, from Beijing to Shijiazhuang. The
692 purple track shows route 2, from Shijiazhuang to Dezhou. The black track shows route 3, from
693 Dezhou to Baoding. The blue track shows route 4, from Cangzhou to Zhuozhou. The yellow track
694 shows route 5, from Zhuozhou to Beijing. The red round dots on the map present the major cities
695 near the routes. The yellow five-pointed stars present the monitoring sites.

Atmos. Chem. Phys. Discuss., doi:10.5194/acp-2016-410, 2016
Manuscript under review for journal Atmos. Chem. Phys.
Published: 24 May 2016

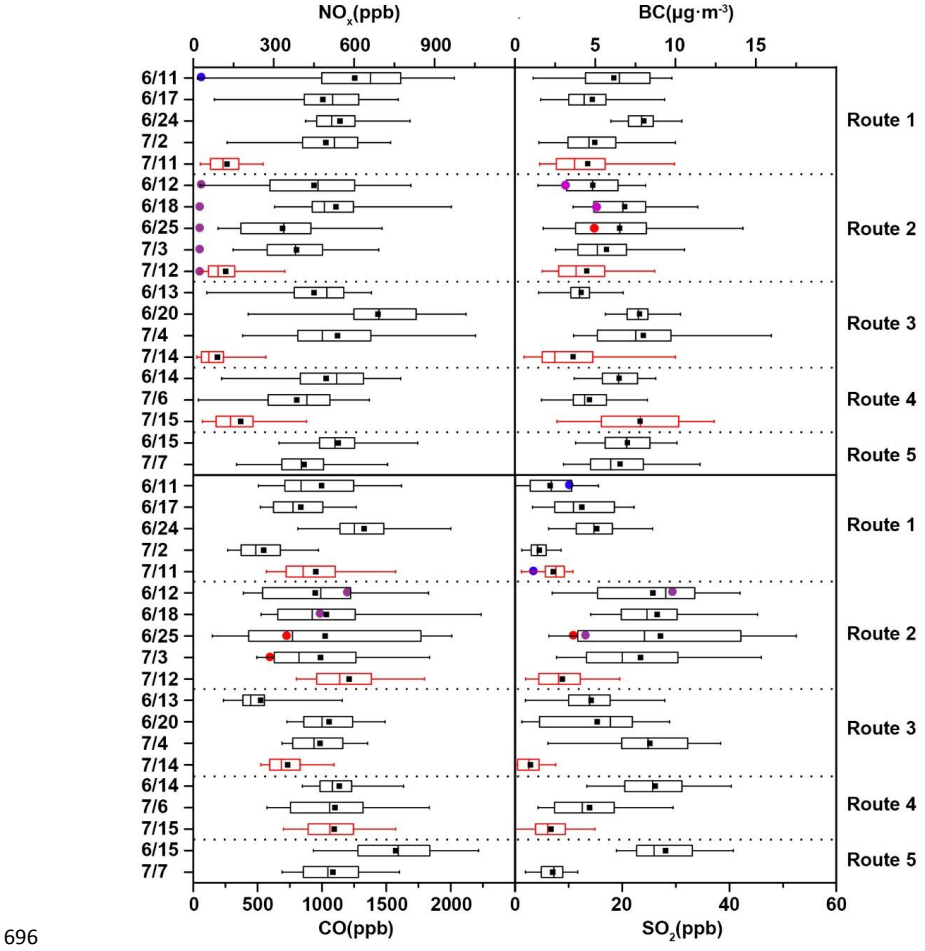

696

697 **Fig. 2.** The concentrations of SO_2, CO, BC and NO_x in each trip in different routes. The red boxes
698 were the results in the last experiment. Values marked were the 5th and 95th percentile (-), standard
699 deviation (lower and upper box lines), median (middle box line), and mean (■). The blue dots
700 were results of GC station. The purple dots were results of QZ station. And the red dots were
701 results of YC station.

Atmos. Chem. Phys. Discuss., doi:10.5194/acp-2016-410, 2016
Manuscript under review for journal Atmos. Chem. Phys.
Published: 24 May 2016

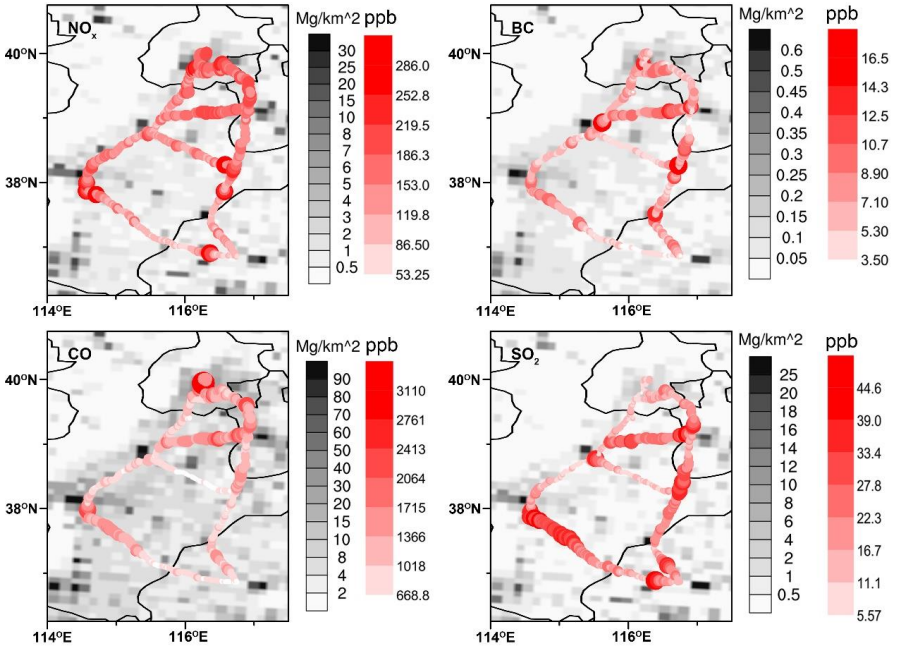

Fig. 3. The spatial distributions of the measured concentrations in our study and the emission maps of SO_2, NO_x, CO and BC. The colored tracks were average concentrations measured in this mobile observation. The black and white maps were emission maps of the year 2010 derived from MEIC model (Zhao et al, 2013).

Atmos. Chem. Phys. Discuss., doi:10.5194/acp-2016-410, 2016
Manuscript under review for journal Atmos. Chem. Phys.
Published: 24 May 2016

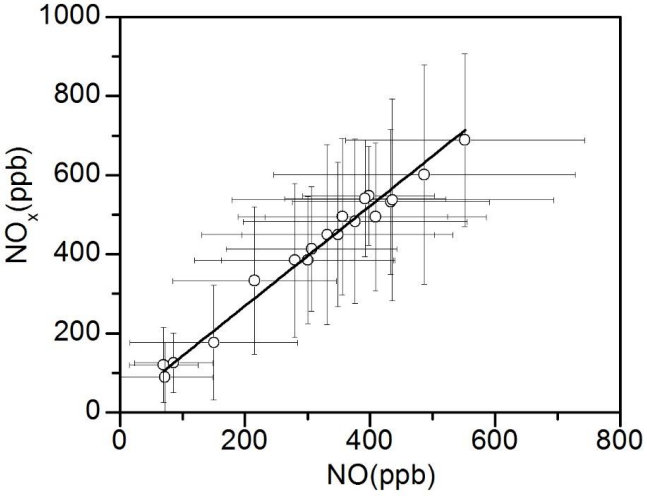

707

708 **Fig. 4.** The regression curve of the means of concentrations of NO_x and NO and the error bars in

709 all 19 trips.

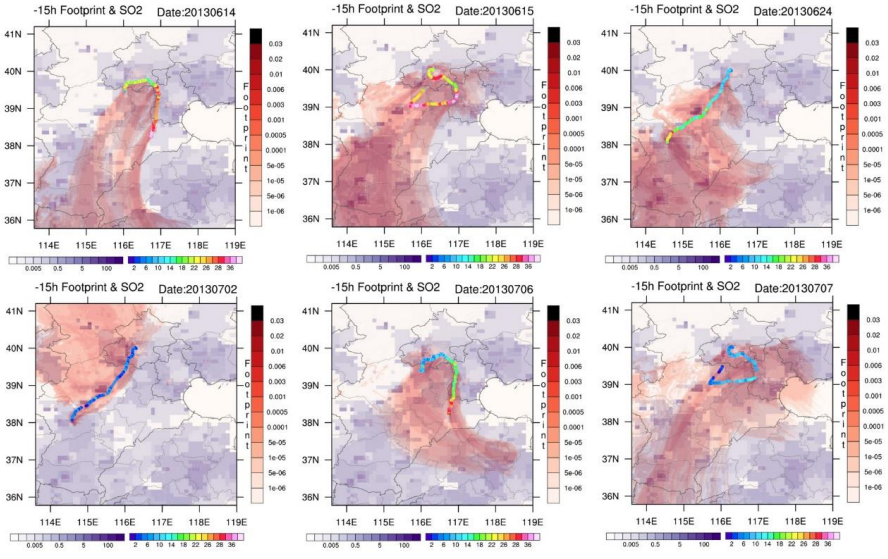

710

711 **Fig. 5.** The back trajectories of observed air masses in the borders of NCP in June 14, June 15,

712 June 24, July 2, July 6 and July 7.

Atmos. Chem. Phys. Discuss., doi:10.5194/acp-2016-410, 2016
Manuscript under review for journal Atmos. Chem. Phys.
Published: 24 May 2016

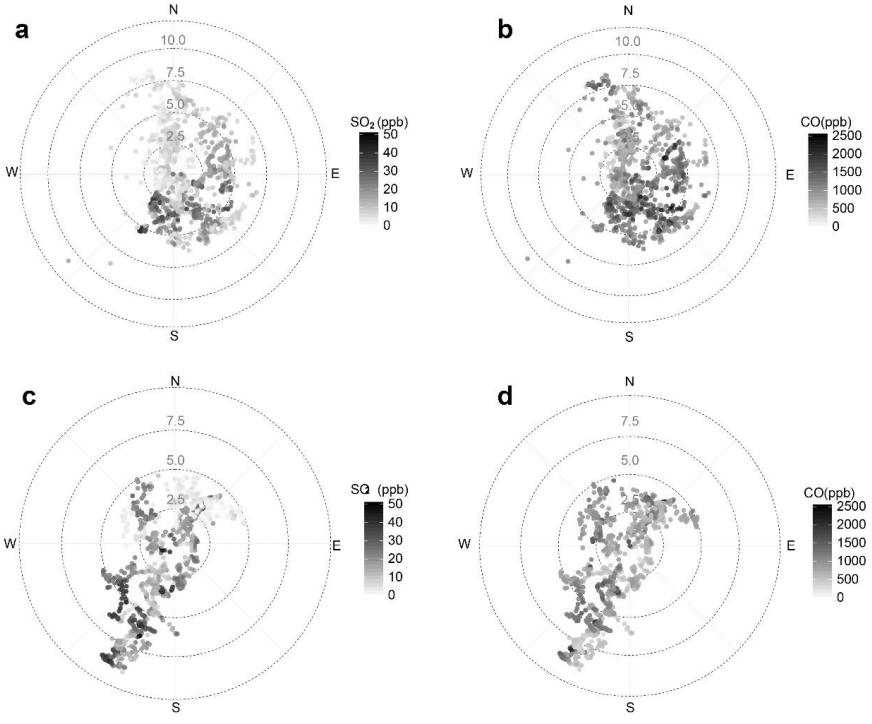

713

714 **Fig. 6.** Wind dependency scatter plots of concentrations of SO_2 and CO in border and central areas

715 in NCP (a. SO_2 in border area; b. CO in border area; c. SO_2 in central area; d. CO in central area).

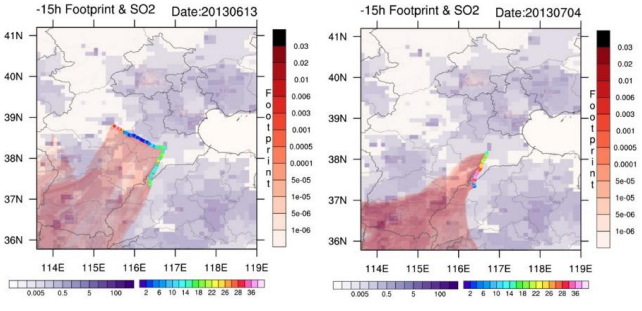

716

717 **Fig. 7.** The back trajectories of observed air masses in the central NCP in June 13 and July 4.